

ICCC 2023 - Guidelines for citation and reuse



Please cite the conference proceedings as following:

Thailand Concrete Association, Ed. *Further Reduction of CO₂ -Emissions and Circularity in the Cement and Concrete Industry, 16th International Congress on the Chemistry of Cement 2023 - ICCC2023* (Bangkok 18.-22.09.2023). Bangkok, 2023. Available at: <https://www.iccc-online.org/archive/>

Please cite individual papers as following:

Author. Title. In: Thailand Concrete Association, Ed. *Further Reduction of CO₂ -Emissions and Circularity in the Cement and Concrete Industry, 16th International Congress on the Chemistry of Cement 2023 - ICCC2023* (Bangkok 18.-22.09.2023). Bangkok, 2023. Available at: <https://www.iccc-online.org/archive/>

All papers in the 2023 conference proceedings are published under the license CC-BY-ND 4.0.

(<https://creativecommons.org/licenses/by-nd/4.0/legalcode>)



Organized by



สมาคมคอนกรีตแห่งประเทศไทย
Thailand Concrete Association



CONGRESS PROCEEDING **VOLUMN III**

Further reduction of CO₂-emission
and circularity in the cement and concrete industry

SEPTEMBER 18-22, 2023

CENTARA GRAND & BANGKOK CONVENTION CENTRE @CENTRALWORLD

Co-Sponsor by



Contact information :

Email: iccc2023.tca@gmail.com

Website : <https://www.iccc2023.org/>

Contents

	Topics	Page
	Preface	i
	Committees	
	- Steering Committee Members	ii
	- Organizing Committee Members	iii
	- Scientific Committee Members	v
	Papers	
PG0001	Utilisation of Polycarboxylate Superplasticiser in Seawater Blended Cementitious Materials: Effect of Superplasticiser Molecular Structure and Seawater Salinity	1
PG0002	Effect of alkanolamines in kaolinitic calcined clays pozzolanic reactivity	6
PG0003	Study to improve vibration flowability of fresh concrete by controlling flocculation state of cement particles	10
PG0004	How does the alternating current field affect the yield stress of fresh cement paste?	14
PG0005	Functionalized transition metal doped silicate hydrate/PCE nanocomposites: an innovative hardening accelerator	19
PG0008	The challenges of combining alkali activation and workability in low carbon binders: a molecular approach	23
PG0012	Interpretation of rheological property of steel slag powder blended cement paste: from interparticle force to physico-chemical parameters	27
PG0014	Influence And Strategies of Plug Flow on The Measured Rheological Properties of Cement-Based Materials	31
PG0016	Effect of the microstructure of polycarboxylate ether (PCE) superplasticizers on the hydration kinetics of Ordinary Portland Cement (OPC)	35
PG0018	C-S-H and pore structure on hardened cement mixed with volcanic glass fine powder	39
PG0022	Early-age workability loss in LC3 systems	43
PG0027	Impact of C-S-H Seeds on Cementitious Hydration Kinetics, Pore Structure, and Early Age Strength	47
PG0028	Influences of Accelerators on the Compressive Strength of Clinker-Efficient Composite Cements with Slag and Limestone	51
PG0031	On the CO ₂ Footprint of Polycarboxylate Superplasticizers (PCEs) and its Impact on the Eco Balance of Concrete	55

Contents

	Topics	Page
PAPERS		
PG0035	A novel formulation concept for fast OPC based tile adhesives	60
PG0036	Hydration and Viscoelastic Properties of Tricalcium Aluminate Pastes Influenced by Soluble Sodium Salts	64
PG0040	Influence of pH value and temperature on the dispersion ability of PCEs containing ethyl acrylate and diethyl maleate segments and its mechanism study	69
PG0041	The Purer the Better: How Monomer Purity Affects the Effectiveness of Phosphate Type Superplasticizers in Cement Paste	73
PG0042	Paste rheology and surface charge of calcined kaolinite	77
PG0043	Rheological properties of belite-calcium sulfoaluminate cement	81
PG0044	Early-age elasticity in structuration of highly cohesive concrete with added pozzolanic diatomaceous earth	85
PG0045	Cellulose ether behavior in slag cement-based tile adhesives	89
PG0046	Influence of key synthetic factors on the molecular characteristics of polycarboxylate superplasticizers	93
PG0049	Influence of retarders on the hydration and rheology of calcium sulfo aluminate cement	97
PG0053	Pore structure of polymer-modified dry mix tile adhesive mortars	101
PG0055	Microscopic tracking of superplasticizer adsorption in alkali activated materials	105
PG0058	Influence of Kaolinite Content on the Fresh Properties of LC ³ Systems	109
PG0059	Non-adsorbing polymers and depletion forces in cement pastes	113
PG0060	Complexation Enthalpies of Organic Admixtures: Measurement Method Development and Application to Calcium Complexes	117
PG0063	Rheology of ultra-high geopolymer concrete: Influences of activator types and silica fume	121
PG0065	Effects of different types of shrinkage reducing agents on shrinkage properties of mortars incorporating slag or silica fume	125

Contents

	Topics	Page
PAPERS		
PG0067	On the impact of sulphate source on admixtures in limestone calcined clay cements	129
PG0071	A study on the adsorption and dispersion capability of PCEs with different structures on cement containing montmorillonite	133
PG0072	Preparation and performance of EPEG-type PCE and its application in ultra-high performance concrete	137
PH0003	Thermal Crack Resistance and DEF Suppression Effect of Concrete Using Fly Ash Cement	141
PH0004	Gradient distribution of slender glass microfibers in 3D printed cementitious filaments	145
PH0005	Effect of Hydrophobically Modified Hollow Glass microspheres on the flow behavior of lightweight high-performance concrete	149
PH0009	Ohmic heating curing for cement-based materials: A promising new technology with enhanced fabrication efficiency	153
PH0011	Preliminary Investigation of 0-3 Lead Zirconate Titanate – Lime Calcined Clay Cement Composites	157
PH0019	New trend line of compressive strength and unit volume weight of cement composites: Lightweight and high-strength at the same time	161
PH0020	Concrete Mix Design for Rigid Pavements Maintenance: Evaluating Compressive Strength Development and Curing Temperature Effect	165
PH0022	Concrete performance with alkali-activated cement based on industrial side streams from Brazil	170
PH0023	Strength Development Prediction and Mixture Optimization of Concrete Used in the Three Gorges Dam	174
PH0024	Inorganic Capsule Based on MgO Expansive Agent for Self-healing Concrete	178
PH0025	Design of High-Performance Concrete (HPC) using calcined clay as supplementary cementitious materials	182
PH0027	The performance of 3D printing PCM concrete with novel hollow ceramsite composite	186

Contents

	Topics	Page
PAPERS		
PH0029	Drying shrinkage and cracks in fresh cement-based materials for 3D printing: an X-Ray Tomograph investigation	190
PH0030	Effect of self-healing on surface morphology in cracked reactive powder concrete	194
PH0034	Sustainable Geopolymer Concrete for Thermoelectric Energy Harvesting	198
PI0002	Various fundamental factors affecting the ion penetration in concrete	202
PI0004	Durability of slag cement and sulfoaluminate cement exposed to acetic acid, ammonium nitrate and magnesium chloride	207
PI0005	Anti-corrosion mechanism of LDHs-VB3- for rebar: insights from experiments and DFT simulations	212
PI0006	Cement use under extreme marine environment–deep sea	216
PI0007	Chloride Adsorption Does Not Retard Chloride Ingress in Concrete	220
PI0008	Roles of slag on corrosion electrochemical measurement in carbonated mortar	224
PI0009	Evaluation of transport properties in ITZ with coupled CT image analysis and simulation	229
PI0012	Assessment of influence of cation type of sulphate ions on early age strength, and microstructure of geopolymer concrete	233
PI0015	Antimicrobial performance of ZnO-modified geopolymer against microbial corrosion	237
PI0017	Cold Water Extraction as a method to determine the free alkali content of cementitious binders	241
PI0020	Understanding the behavior of magnesium potassium phosphate cements under leaching	245
PI0023	Effect of Al on the structure and swelling behavior of synthetic ASR gels	250
PI0025	Geochemical interactions between cementitious materials and water in the context of drinking water supply	254
PI0026	Restraint effect of steel bar on cement-based materials at early age : A full cross section study	258
PI0029	Effect of Sulfate Attack on the Cement Mortars and Pastes with Different Replacement Levels of Limestone at a Low Temperature	262

Contents

	Topics	Page
PAPERS		
PI0031	Alkali-silica reaction resistance of alkali-activated calcined clays using accelerated mortar bar test	266
PI0032	Investigation on the durability evolution of high belite cement subjected to thermal fatigue	270
PI0034	Research on the leaching mechanism of C-S-H : experiments and molecular dynamics simulations study	274
PI0035	The deterioration process of alkali activated slag exposed to sulfate attack and calcium leaching	278
PI0037	Multiphysics discrete modeling for expansion and deterioration of concrete due to alkali-silica reaction	282
PI0039	Kinetics of iron (hydr)oxide precipitation in cementitious materials	287
PI0040	Preparation of (super)hydrophobic cement-based matrix with organosiloxanes and micromodification of the surface	292
PI0041	Assessment of the ion diffusivity of cement-based materials using QXRD and micro-CT based random walk simulation	296
PI0043	Effect of Mg-bearing water on the chemical and mechanical properties of a low C/S industrial cement paste	300
PI0044	Corrosion kinetics of steel in artificial carbonated pore solutions under the effect of stirring and bicarbonate ions	304
PI0047	Chloride ingress resistance of Ca(OH) ₂ activated GGBFS: Impact of curing temperature and additional activators	308
PI0048	A new unidirectional testing approach for sulfate resistance on cement mortars	312
PI0049	A comparative assessment of different additives to reduce carbonation degradations of alkali-activated slag using in-situ ftir technique	316
PI0050	Appraisal of the microstructural properties of ASR affected concrete at different moisture conditions using the DRI	320
PI0052	Property changes of calcium sodium aluminosilicate hydrates (C-NA-S-H) gels subjected to water immersion	324
PI0056	Experimental investigation of expansion and damage due to alkali-silica reaction at low temperature	328
PI0057	Physicochemical stability of calcium aluminate cement and hemihydrate-based material exposed to deep sea	332

Contents

	Topics	Page
PAPERS		
PI0060	Resistance against chloride and carbonation of binary and ternary binder with GGBS or/and limestone	336
PI0061	The fate of ferrous ions in corroding steel reinforced concretes	340
PI0065	Effect of waterproofing chemicals on carbonation in Low clinker cement with pore structure analysis	344
PI0066	The square root law with an offset applied to chloride diffusion in slowly reacting blended cement pastes	348
PI0067	Phase Evolution and Property Development of Alkali-Silica Reaction Gel in Carbonation	352
PI0068	L-Ascorbic Acid used as green corrosion inhibitor in chloride-bearing steel reinforced cement mortars	356
PI0070	Carbonation of Concrete with SCMs: a data analysis by RILEM TC 281-CCC	360
PI0073	Towards the Development of Prescriptive-Based Specifications for Non-Traditional SCMs to Prevent Alkali-Silica Reaction	364
PI0074	Elucidating the carbonation front in blended calcined kaolinite clays binders using analytical techniques	368
PI0078	Cementitious materials for oil-well abandonment and numerical simulations of cement durability at oil well conditions	372
PI0081	Alkali-silica reaction in calcium aluminate cement mortars	377
PI0084	AAM – oil composite: a new highly durable material with a negative carbon footprint	381
PI0086	Coefficient of thermal expansion of alkali-activated slag concrete	386
PI0090	Study on the Deterioration Mechanism of Cementitious Waterproofing Membrane (Part I: Macroscopic Performance)	390
PI0091	Impact of an evolving microstructure on the square-root law for chloride ingress	395
PI0092	Formation Factor as a Non-Destructive Measure of Chloride Diffusion Coefficient	399
PI0098	Surface effect on chloride diffusion in calcium silicate hydrate	403
PJ0001	Preparation of reactive urchin-like recycled concrete aggregate by wet carbonation: towards improving the bonding capability	407

Contents

	Topics	Page
PAPERS		
PJ0002	Physical and mechanical characterization of Alkali-Activated slag cement in presence of ion-exchange resins	411
PJ0005	Evaluation of environmental technologies for cement production considering multiple environmental categories	415
PJ0011	Structure and Reactivity of Aqueous Carbonated Blended Cement Pastes	419
PJ0013	Statistical modelling and optimization of strength in hybrid binders based on volcanic pumice, environmental and cost analysis.	423
PJ0014	CDW waste as retardants of ions harmful to cement	428
PJ0016	Production of a hydraulic material from post treated steelmaking slags	432
PJ0020	Influence of sisal fiber on mechanical, shrinkage and high temperature performance of UHPC	437
PJ0023	Acid activation of phosphate by-products in geopolymerization technology	442
PJ0027	Sulfate Resistance of Mortar Containing Low-Grade Calcined Clay	447
PJ0029	The role of $C_{12}A_7$, α' H- C_2S and dehydrated amorphous nesosilicate in rehydration of recycled cement	452
PJ0031	Carbonation and hydration kinetics of CO_2 injected ready-mixed concrete	456
PJ0033	Assessment of the Microstructure and Mass Transfer in Strontium-Loaded Geopolymer Cement Wasteforms	460
PJ0034	Pretreatments processes of alkaline recycled concrete aggregates to maximize CO_2 capture in accelerated carbonation processes.	464
PJ0041	Effect of Manganese Sulfate Replacing Gypsum on Properties and Reducing Cr(VI) of Cement Paste	468
PJ0048	Study on MSWI fly ash solidifiers based on product composition design	472
PJ0050	An Experimental Study of Sulfur and Chlorine Stripping from Cement Hot Meal	476
PJ0052	Effect of copper tailing powder on the hydration and mechanical properties of concrete under low atmospheric pressures	480

Contents

	Topics	Page
PAPERS		
PJ0056	Mineralogical Characterization of Waste to Energy (WTE) Ashes - Insights from Raman Imaging	484
PJ0057	Recycling of phosphate waste rocks to produce alkali-activated mortars	488
PJ0059	Effect of strontium salts on the kinetics and mechanisms of geopolymer cement formation	493
PJ0062	Developing Pickering emulsion routes towards oil immobilisation in geopolymers	497
PJ0064	Developing circular concrete through acid leaching of waste fines	501
PJ0065	Application of Recycled Cementitious Material from Concrete Waste for UK Nuclear Waste Encapsulation	506
PJ0067	Investigation on the effect of recycled powders from demolished concrete on the rheological properties of cement paste	510
PJ0068	Evaluating the potential of Steel slags as alternative raw materials for Portland cement clinker production	515
PJ0069	Upcycling of bio-waste ashes into additive for concrete	519
PJ0071	Decarbonizing UAE Cement Industry with Limestone Calcined Clay Cement (LC ³)	523
PJ0074	Development of a CO ₂ mineralization technology for concrete wash water upcycling	528
PJ0075	Properties of a Magnesium-Silicate-Hydrate Cement Paste Prepared Using Magnesium Hydroxide	532
PJ0078	Influence of Rice Husk on the Thermal Activation and Pozzolanic Activity of Tropical Soils	536
PJ0080	Effect of Mix Proportion as W/C and Amount of GGBS Contents on CO ₂ Adsorption	541
PJ0081	Use of concrete slurry waste as an accelerator - Effect on early-age strength development and hydration of steam-cured specimen	545
PJ0082	A Study on Mortar Properties Focusing on Water Absorption Ratio of Carbonated Recycled Fine Aggregate	549
PJ0083	Effect of Conditions on Pore structure of silica gel in Wet Carbonated Recycled Cement Paste Powder	553

Contents

	Topics	Page
PAPERS		
PJ0084	Aqueous Carbonation of Recycled Concrete Fines: Towards Higher Efficiency	557
PJ0085	Study on the Use of Recycled Aggregates for the Production of Cementless Pervious Concrete	561
PJ0087	Eco-toxicity assessment of cement. Bioassays on luminescent bacteria and sea urchin embryogenesis	565
PJ0090	Influence of low carbon cement and recycled aggregates on mortar fresh state and early hydration	569
PJ0091	Rehydration of ettringite: microstructure and mechanical properties	573
PJ0092	Physical Properties of Biochar Enhance the Rheological Behavior of Cement-Based Materials	578
PJ0093	The reactivity of hydrothermally activated basic oxygen furnace slag	583
PJ0095	Optimization of low clinker limestone calcined clay cement (LC ³) concrete mixes as further carbon footprint reduction strategy	588
PJ0097	Research on multi-solid waste co-excitation of lead smelting slag to prepare green filling materials for mines and its performance	592
PJ0105	Effects of phosphate salts on the interfacial bonding between magnesium phosphate cement and steel fiber	596
PJ0114	Formation of closed pore structure porous glass-ceramics for thermal insulation	600
PJ0116	Carbonation effects on mechanical performance and microstructure of LWAs produced with hydrated cement paste powder	604
PK0001	Study for New Japanese Industrial Standards; “Volcanic Glass Powder for Use in Concrete”	609
PK0002	Cement types and seawater exposure in Europe – implications for infrastructure and its integration into marine habitats	613
PK0004	Effect of water content on fluorescence intensities of cement-based materials	617
PK0005	A micromechanical modelling approach to study the effect of shape of hydrates on creep properties of cement pastes	621

Production of a hydraulic material from post treated steelmaking slags

K. Schraut^{1*}, B. Adamczyk², C. Adam³, D. Stephan⁴, S. Simon⁵, J. von Werder⁶, and B. Meng⁷

¹ Bundesanstalt für Materialforschung und -prüfung (BAM), Berlin, Germany
Email: katharina.schraut@bam.de

² Bundesanstalt für Materialforschung und -prüfung (BAM), Berlin, Germany
Email: burkart.adamczyk@bam.de

³ Bundesanstalt für Materialforschung und -prüfung (BAM), Berlin, Germany
Email: christian.adam@bam.de

⁴ Technische Universität Berlin, Berlin, Germany
Email: stephan@tu-berlin.de

⁵ Bundesanstalt für Materialforschung und -prüfung (BAM), Berlin, Germany
Email: sebastian.simon82@gmail.com

⁶ Bundesanstalt für Materialforschung und -prüfung (BAM), Berlin, Germany
Email: Julia.von-Werder@bam.de

⁷ Bundesanstalt für Materialforschung und -prüfung (BAM), Berlin, Germany
Email: Birgit.Meng@bam.de

ABSTRACT

Steelmaking slag is a by-product of steel production, of which 4.5 Mt were produced in 2020 in Germany alone. It is mainly used in road construction, earthwork and hydraulic engineering. A smaller part is returned to the metallurgical cycle, used as fertiliser or landfilled.

With this use, iron oxides still contained in steelmaking slag are lost. In addition, the possibility of producing higher-grade products from steelmaking slag is foregone. In recent decades, many researchers have investigated the production of Portland cement clinker and crude iron from basic oxygen furnace slags (BOFS) via a reductive treatment. Carbothermal treatment of liquid BOFS causes a reduction of iron oxides to metallic iron, which separates from the mineral phase due to its higher density. Simultaneously, the chemical composition of the reduced slag is adapted to that of Portland cement clinker.

In this study, German BOFS was reduced in a small-scale electric arc furnace using petrol coke as a reducing agent. The resulting low-iron mineral product has a similar chemical composition to Portland cement clinker and was rich in the tricalcium silicate solid solution alite (Ca₃SiO₅). Based on its chemical and mineralogical composition, similar to that of Portland cement clinker, the reduced BOFS has the potential to react comparably. In our study, the reduced BOFS produced less hydration heat than OPC, and its hydraulic reaction was delayed. However, adding gypsum has shown to accelerate the hydration rate of the reduced BOFS compared to that known from the calcium silicates of Portland cement clinker. Further research to improve the hydraulic properties of the reduced slag is essential. If successful, producing a hydraulic binder and crude iron from BOFS has economic and ecological benefits for both the cement and steel industries.

KEYWORDS: *steelmaking slag, alite, hydraulic reactivity, clinker substitute*

1. Introduction

Basic oxygen furnace slags (BOFS) contain 7–50 wt.% Fe₂O₃, 31–56 wt.% CaO, 10–27 wt.% SiO₂, 1–4.5 wt.% Al₂O₃, 0.3–10 wt.% Mn₂O₃, and 0.8–15 wt.% MgO (Menad et al., 2014). Despite their high basicity (CaO/SiO₂ ratio) and a content of up to 20 wt.% alite (Ca₃SiO₅) and up to 60 wt.% belite (β-Ca₂SiO₄) (Das et al., 2007), BOFS are scarcely used for cement production due to their high iron oxides content, low content of hydraulic phases, and content of up to 15 wt.% free CaO and 5 wt.% MgO, which make BOFS a risk for volume instability (Das et al., 2007, Waligora et al., 2010, Menad et al., 2014).

In the past, several different ways to produce a hydraulic or pozzolanic material from BOFS have been investigated, e.g. (Li et al., 2011, Belhadj et al., 2012, Ludwig and Wulfert, 2012, Li et al., 2013, Neto et al., 2017, Liu et al., 2019). A reductive treatment of BOFS as described in (Kubodera et al., 1979, Piret and Dralants, 1984, Dziarmagowski et al., 1992, Reddy et al., 2006, Ludwig and Wulfert, 2012, Wulfert et al., 2013a, Wulfert et al., 2013b, Liu et al., 2017) is advantageous because it allows both the recovery of iron from the BOFS and the simultaneous production of Portland cement clinker. The properties of the final hydraulic product depend on the composition of the original BOFS, the degree of reduction, and the modifications made during the treatment.

However, it was found that the hydraulic reaction of the Portland cement clinker-like material produced from BOFS was significantly delayed compared to ordinary Portland cement (OPC) (Schraut et al., 2021). Since OPC is a product of finely ground cement clinker mixed with a certain amount of calcium sulfates, such as gypsum ($\text{CaSO}_4 \cdot 2\text{H}_2\text{O}$), the next step was to investigate the hydraulic reactivity of the clinker-like material from BOFS with the addition of gypsum. Besides controlling the tricalcium aluminate reaction, calcium sulfates also accelerate the hydration of calcium silicates (Bentur, 1976, Quennoz and Scrivener, 2013) and increase the dissolution of alite (Menetrier et al., 1980).

To keep the complexity of the system low, the addition of calcium sulfates other than gypsum has been refrained from in this study.

2. Materials and Methods

A BOFS from a German steel plant was used for the thermochemical experiments. The slag was crushed to a maximum grain size of approx. 20 mm and dried at 200 °C before it was molten and reduced in the small technical scale electric arc furnace of the Bundesanstalt für Materialforschung und -prüfung (BAM). The electric arc furnace has a power of 480 kW and is equipped with three graphite electrodes with a diameter of 60 mm. The experiments were conducted in a graphite-lined furnace vessel with a volume of approx. 0.4 m³. 58 g of petrol coke per kg of BOFS was added as a reducing agent. The generated metallic iron was sedimented at the bottom of the furnace and was obtained manually after cooling. Cooling took place in the reactor within ~24 h. For more details, see Schraut et al. (2021).

The chemical composition of the samples was determined by CRB Analyse Service GmbH on fused beads by X-ray fluorescence analysis (XRF). The crystalline phase composition was determined by X-ray diffraction (XRD) with a Bruker D8 Advance X-ray diffraction system at 40 kV and 40 mA over an angular range of 5–85 °2θ with a step size of 0.02 °2θ and a velocity of 2 s/step. The instrument was equipped with a Cu-tube, a LynxEye XE-T detector, and a fixed slit (0.3°). To investigate the crystalline hydrates with XRD, the hydration was stopped after 2, 7, 14, 28, 56, and 90 d using the solvent exchange method with isopropanol.

The hydration heat was measured over two weeks in an isothermal calorimeter TAM Air 8-channel from TA instruments at a temperature of 20 °C. 3 g of the ground sample was externally mixed for 1 min with 1.5 g distilled water resulting in a water-to-binder (W/B)-ratio of 0.5.

As a reference, a commercial CEM I 32.5 R from Schwenk Zement KG was prepared and analysed under the same conditions as the experimental samples. Gypsum (EMSURE® p.A. from Merck KGaA) was added to the sample in a concentration corresponding to 1.0 wt.% SO₃.

3. Results and Discussion

The reductive treatment resulted in a transformation of the oxide-bound iron in brownmillerite ($\text{Ca}_2(\text{Al,Fe})_2\text{O}_5$), wuestite (FeO) and magnetite (Fe_3O_4) to metallic iron, which separated from the mineral slag. Accordingly, the mass fraction of Fe₂O₃ in the mineral slag (reduced BOFS) decreased from about 29 wt.% to about 6 wt.%, while the mass fractions of CaO and SiO₂ increased proportionally (Table 1). The mineralogical composition of the reduced BOFS changed correspondingly. While the Fe-oxides and Fe-Al-oxides disappeared, alite formed the new main mineral phase in the reduced BOFS. Besides alite, belite, mayenite ($\text{Ca}_{12}\text{Al}_{14}\text{O}_{33}$), tricalcium aluminate ($\text{Ca}_3\text{Al}_2\text{O}_6$), portlandite ($\text{Ca}(\text{OH})_2$) and periclase (MgO) were identified in the reduced BOFS as crystalline phases. Therefore, it can be stated that the mineralogical and chemical composition of the reduced BOFS is close to the mineralogical and chemical composition of Portland cement clinker.

The formation of alite in reduced BOFS was also reported by Kubodera et al. (1979), Wulfert et al. (2013b) and Dziarmagowski et al. (1992) and is likely to depend on the CaO/SiO₂-ratio of the reduced slag. Alite was identified as the main mineral in reduced BOFS with CaO/SiO₂ > 2.9, while belite was the main mineral in reduced BOFS with CaO/SiO₂ < 2.6 (Dziarmagowski et al., 1992, Reddy et al., 2006).

Table 1: Chemical composition of the original BOFS, the reduced BOFS (rBOFS), and a commercial OPC CEM I 32.5 R (CEM I) determined by XRF. All mass fractions are given as wt.% oxides, although this may not always represent the actual oxidation state of each element in the samples. Only element oxides whose mass fractions were > 0.1 wt.% in at least one sample are shown.

[wt.%]	CaO	SiO ₂	Fe ₂ O ₃	MnO	MgO	Al ₂ O ₃	P ₂ O ₅	Cr ₂ O ₃	TiO ₂	V ₂ O ₅	SO ₃	SrO	Na ₂ O	K ₂ O
BOFS	43.48	12.07	28.59	4.554	3.64	1.79	1.12	0.518	0.524	0.310	0.23	0.025	0.07	<0.03
rBOFS	64.00	19.54	5.64	3.151	3.15	2.53	1.20	0.419	0.730	0.399	0.05	0.035	<0.06	<0.03
CEM I	61.97	19.36	3.06	0.047	3.04	4.96	0.44	0.013	0.322	0.010	3.03	0.148	0.21	0.92

The main hydration reaction of the reduced BOFS was considerably slower than that of OPC and started only after ~9 d of hydration (Figure 1). The hydration heat maximum was reached after about 14 d of hydration. The cumulative heat of hydration after 14.5 d was ~90 J/g. The first hydrates to form were portlandite (Ca(OH)₂) and brucite (Mg(OH)₂). Additionally, hemicarboaluminate ([Ca₄Al₂(OH)₁₂][OH(CO₃)_{0.5}·4H₂O]) was detected and transformed later to carbonated hemicarboaluminate ([Ca₄Al₂(OH)₁₂][OH_{0.4}(CO₃)_{0.8}·4H₂O]) and monocarboaluminate (Ca₄Al₂(OH)₁₂(CO₃)·5H₂O). The addition of 1 wt.% SO₃ in the form of gypsum accelerated the reaction of the reduced BOFS significantly. The main hydration reaction started after ~1 d of hydration and the cumulative heat of hydration after 14.5 d increased to ~160 J/g. Furthermore, the heat flow curve showed a sharp peak after ~2 d and 5 h that can be interpreted as the reaction peak of the aluminate reaction. Since the aluminate reaction occurred after the silicate reaction, the sample can be considered properly sulfated (Quennoz and Scrivener, 2013). In rBOFS + 1 wt.% SO₃, ettringite formed besides portlandite and brucite. No carboaluminates formed during hydration of rBOFS + 1 wt.% SO₃.

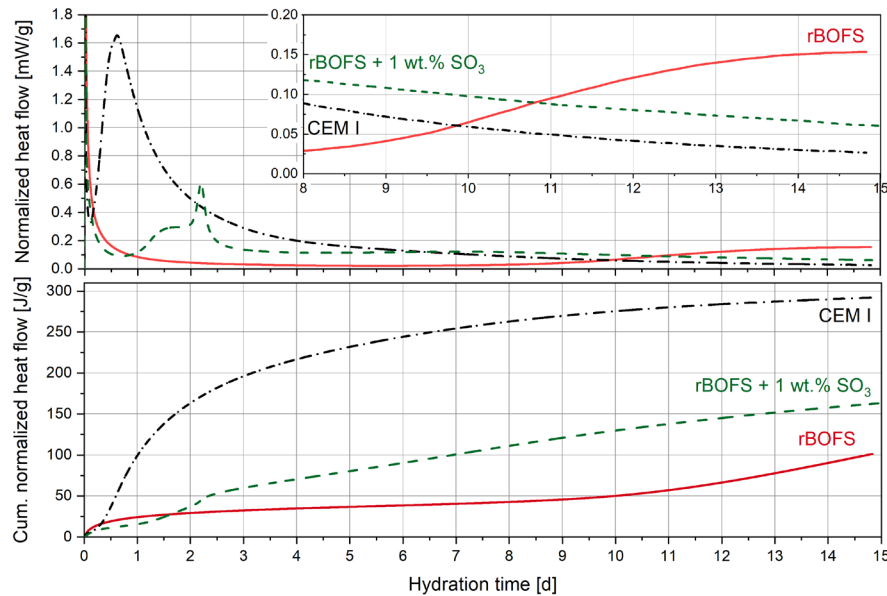


Figure 1: Normalised heat flow and cumulative normalised heat of the reduced BOFS (red, solid line), the reduced BOFS with the addition of an equivalent of 1 wt.% SO₃ as gypsum (green, dashed line) and of a commercial CEM I (black, dash-dotted line) measured for 14.5 d.

Sulfate is known to influence the silicate reaction. An accelerated dissolution of the alite with addition of sulfates was reported by (Bentur, 1976, Menetrier et al., 1980, Zajac et al., 2014, Bergold et al., 2017, Zunino and Scrivener, 2020, Andrade Neto et al., 2022). The reasons for this are still debated. The effect

was proposed to be caused by a promotion of C-S-H growth by ettringite acting as additional nuclei (Bergold et al., 2017, Tan et al., 2019) or by a change in C-S-H morphology (Andrade Neto et al., 2022). Other researchers assumed that a decrease of Ca^{2+} activity due to the formation of CaSO_4^0 species or an increased protonation of the C_3S surface by sulfate ions enhances the alite dissolution (Nicoleau et al., 2014). The binding of Al ions as ettringite is most likely not the causative agent, as acceleration by gypsum was observed in C_3S with and without Al (Andrade Neto et al., 2022).

4. Conclusions

The reductive treatment of BOFS can be used to recover iron from BOFS while simultaneously producing a material similar to Portland cement clinker. The majority of iron was reduced to metallic iron and separated from the mineral melt. The reduced BOFS had a chemical and mineralogical composition close to that of Portland cement clinker and contained alite as the main mineral.

The reduced BOFS reacted considerably more slowly with water than OPC. However, the reaction rate was increased with the addition of gypsum. Further investigations are needed, including using different sulfate carriers and SO_3 contents, to determine the actual mechanisms behind this acceleration. Nevertheless, the reduced BOFS shows potential as a cement component or concrete addition contributing to long-term hardening.

Acknowledgements

We would like to thank I. Feldmann for SEM pictures, D. Al-Sabbagh for XRD measurements and T. Hirsch for calorimetric measurements.

This work was funded by the German ministry of Education and Research (BMBF) under the funding guideline „Resource-efficient circular economy - Building and mineral cycles (ReMin)“ funding number 033R254A.

References

- Menad, N., Kanari, N. and Save, M. (2014) "Recovery of high grade iron compounds from LD slag by enhanced magnetic separation techniques", *International journal of mineral processing*, 126: 1-9
- Das, B., Prakash, S., Reddy, P. and Misra, V. (2007) "An overview of utilization of slag and sludge from steel industries", *Resources, Conservation and Recycling*, 50(1): 40-57
- Waligora, J., Bulteel, D., Degrugilliers, P., Damidot, D., Potdevin, J. and Measson, M. (2010) "Chemical and mineralogical characterizations of LD converter steel slags: A multi-analytical techniques approach", *Materials characterization*, 61(1): 39-48
- Li, J., Yu, Q., Wei, J. and Zhang, T. (2011) "Structural characteristics and hydration kinetics of modified steel slag", *Cement and Concrete Research*, 41(3): 324-329
- Belhadj, E., Diliberto, C. and Lecomte, A. (2012) "Characterization and activation of basic oxygen furnace slag", *Cement and concrete composites*, 34(1): 34-40
- Ludwig, H. and Wulfert, H. (2012) 18. *Int. Baustofftagung ibausil*, pp. 18-25. Weimar
- Li, Z., Zhao, S., Zhao, X. and He, T. (2013) "Cementitious property modification of basic oxygen furnace steel slag", *Construction and Building Materials*, 48: 575-579
- Neto, J.B.F., Fredericci, C., Faria, J.O., Chotoli, F.F., Ribeiro, T.R., Malynowskyj, A., Silva, A.L., Quarcioni, V.A. and Lotto, A.A. (2017) "Modification of Basic Oxygen Furnace Slag for Cement Manufacturing", *Journal of Sustainable Metallurgy*, 3(4): 720-728
- Liu, C., Huang, S., Blanpain, B. and Guo, M. (2019) "Effect of Al_2O_3 Addition on Mineralogical Modification and Crystallization Kinetics of a High Basicity BOF Steel Slag", *Metallurgical and Materials Transactions B*, 50(1): 271-281
- Kubodera, S., Koyama, T., Ando, B. and Kondo, R. (1979) "An approach to the full utilization of LD slag", *Transactions of the Iron and Steel Institute of Japan*, 19(7): 419-427
- Piret, J. and Dralants, A. (1984) "Utilization of LD Process Slag for the Production of Portland Cement Clinker and Pig Iron", *Stahl und Eisen*, 104(16): 774-778
- Dziarmagowski, M., Karbowniczek, M., Pyzalski, M. and Okon, J. (1992) "Reduction of converter slag in electric arc furnace", *Ironmaking & steelmaking*, 19(1): 45-49
- Reddy, A.S., Pradhan, R. and Chandra, S. (2006) "Utilization of basic oxygen furnace (BOF) slag in the production of a hydraulic cement binder", *International journal of mineral processing*, 79(2): 98-105

- Wulfert, H., Keyssner, M., Ludwig, H. and Adamczyk, B. (2013a) "Metal recovery and conversion of steel slag into highly reactive cement components/Metallgewinnung und Umwandlung von LD-Schlacke in hochreaktive Zementkomponenten", *ZKG international*, 9: 34-40
- Wulfert, H., Keyßner, M., Ludwig, H., Adamczyk, B. and Schiffers, A. (2013b) "Hochreaktive Zementkomponenten aus Stahlwerksschlacken verbessern Ökologie und Ökonomie/ Highly reactive cement components from steel slag for optimized ecology and economy", *Stahl und Eisen*, 133(12): 45-50
- Liu, C., Huang, S., Wollants, P., Blanpain, B. and Guo, M. (2017) "Valorization of BOF steel slag by reduction and phase modification: metal recovery and slag valorization", *Metallurgical and Materials Transactions B*, 48(3): 1602-1612
- Schraut, K., Adamczyk, B., Adam, C., Stephan, D., Meng, B., Simon, S. and von Werder, J. (2021) "Synthesis and characterisation of alites from reduced basic oxygen furnace slags", *Cement and Concrete Research*, 147: 106518
- Bentur, A. (1976) "Effect of Gypsum on the Hydration and Strength of C₃S Pastes", *Journal of the American Ceramic Society*, 59(5- 6): 210-213
- Quennoz, A. and Scrivener, K.L. (2013) "Interactions between alite and C₃A-gypsum hydrations in model cements", *Cement and Concrete Research*, 44: 46-54
- Menetrier, D., Jawed, I. and Skalny, J. (1980) "Effect of gypsum on C₃S hydration", *Cement and Concrete Research*, 10(5): 697-701
- Zajac, M., Rossberg, A., Le Saout, G. and Lothenbach, B. (2014) "Influence of limestone and anhydrite on the hydration of Portland cements", *Cement and concrete composites*, 46: 99-108
- Bergold, S., Goetz-Neunhoeffler, F. and Neubauer, J. (2017) "Interaction of silicate and aluminate reaction in a synthetic cement system: Implications for the process of alite hydration", *Cement and Concrete Research*, 93: 32-44
- Zunino, F.A. and Scrivener, K. (2020) "Factors influencing the sulfate balance in pure phase C₃S/C₃A systems", *Cement and Concrete Research*, 133: 106085
- Andrade Neto, J.S., Rodríguez, E.D., Monteiro, P.J., De la Torre, A.G. and Kirchheim, A.P. (2022) "Hydration of C₃S and Al-doped C₃S in the presence of gypsum", *Cement and Concrete Research*, 152: 106686
- Tan, H., Li, M., Ren, J., Deng, X., Zhang, X., Nie, K., Zhang, J. and Yu, Z. (2019) "Effect of aluminum sulfate on the hydration of tricalcium silicate", *Construction and Building Materials*, 205: 414-424
- Nicoleau, L., Schreiner, E. and Nonat, A. (2014) "Ion-specific effects influencing the dissolution of tricalcium silicate", *Cement and Concrete Research*, 59: 118-138